Increasing Mobile Robot Tethered Payload Transport Capacity Through Multipurpose Manipulation

Raymond Kim[1], Edward Diller[1], Eemil Harkonen[1], Anirban Mazumdar[1]

Abstract—Mobile robots can pull payloads far greater than their mass. However, off-road terrain features substantial variation in height, grade, and friction. In addition, temperature changes and precipitation add a time-varying element to the terrain. These effects can cause traction to degrade or fail catastrophically. To maximize tethered payload transport capacity through optimal vehicle traction, unique solutions are required for each surface/condition. This paper presents a system that utilizes a vehicle-mounted, multipurpose manipulator to physically adapt the robot with unique anchors suitable for a particular terrain for autonomous payload transport. Specifically, this work presents "swappable anchors", which can be easily attached/detached to adapt the vehicle using permanent magnets. We present four unique anchor designs, each optimal for a specific surface, and experimentally validate them. The experimental results illustrate how this approach can increase the overall payload capacity of a system on various surfaces by increasing the effective coefficient of friction. We demonstrate how we can use the manipulator to autonomously localize the payload using a visual sensor, attach the payload to the vehicle using a permanent-magnet-based payload key/lock, and enable versatile payload transport capacity.

Index Terms—Modeling and Design of Mechatronic Systems, Mobile Robots, Vehicles and Space Exploration

I. INTRODUCTION

Mobile robots can transport large payloads in various environments to improve search and rescue missions and planetary exploration. Outdoor, unstructured, or extra-planet environments often feature diverse terrain with a range of hardness, texture, and wetness. Different surfaces often require unique traction methods. For example, gecko-adhesives perform well on smooth clean surfaces [1] while microspines thrive on hard rough surfaces [2]. In environments with diverse conditions, payload-transport robots must be able to autonomously optimize traction across diverse conditions.

This work presents a manipulation-driven adaptation for autonomous payload transport across various terrain. Specifically, we propose a mobile robot system that can carry a range of traction mechanisms that can be deployed/removed using an on-board multi-purpose manipulator. This paper illustrates how the vehicle-mounted manipulator can be used to physically adapt the system with unique anchors to increase the overall effective coefficient of friction on a specific surface. This capability can ensure high vehicle traction of a system across various surfaces for payload transport. The key contributions of this paper are 1) creating a permanent-magnet-based mechanical design for swappable anchors, 2) illustrating how swapping anchors using a manipulator can increase the coefficient of friction between the vehicle and

Fig. 1. (1) Vehicle-mounted manipulator can localize and attach the payload to the vehicle. (2) An anchoring device can be engaged on a given surface to increase payload capacity. (3) The anchoring device can be swapped using the manipulator for a different surface. (4) The robot can pull the payload on a different surface using a different anchor.

the given surface, 3) and experimentally demonstrating the ability to transport loads up to $38\times$ the robot mass on various surfaces through multi-purpose manipulation and swappable anchors. Figure 1 illustrates how manipulation can be used to enable physical adaptations for autonomous payload transport on various surfaces.

II. RELATED WORKS

Currently, many innovative solutions exist that increase vehicle traction for payload transport on different types of surfaces. On flat, smooth surfaces, adhesive pads have been shown to enable adhesion for mobility and payload transport [3]. Similarly, gecko-inspired adhesives on microbots have demonstrated the ability to pull loads at human scale forces [1], [4]. The overall application of adhesives has been focused on small, microbots and their size entails limited mobility, restricting them to unobstructed, flat, and smooth environments.

On hard, rough surfaces, various solutions have been introduced in the field. Rovers with high-speed vacuum suction modules have been presented to provide high load-carrying capacity [5]–[7], but at the cost of significant noise and reduced speed. Legged robots have also been shown to pull heavy payloads on paved asphalt [8], [9], but they require actuation and power to fully engage traction with the given terrain. Microspines are alternate solutions that offer high friction on rough surfaces with asperities. These works demonstrate the benefit of multiple microspines for load sharing and scaling steep, vertical surfaces with high shear forces

and little, or even negative, normal forces [2], [10]–[12]. Microspines have also been used in applications for gripping and anchoring to increase the overall payload capacity of the system by providing counter-reactionary forces in multiple directions [13]–[15]. While microspines have proven to be very effective on rugged terrains with asperities, they suffer on softer, more granular terrain [16].

On soft, granular surfaces, tail-based anchoring robots have been developed to pull heavy payloads by exploiting winch tension and plowing [17]. Mud is also known as a common failure mode for wheeled vehicles, and the literature currently has no clearly optimal solution for traction in mud.

While optimal solutions exist for a range of terrain, such optimal solutions can fail dramatically when used on different terrain. Therefore, there is a need for multi-purpose or adaptive systems. A recent publication demonstrated a microspine-rubber composite that could be used for multipurpose traction on both smooth and rough surfaces that can support large loads with a high coefficient of friction [18]. In contrast, adaptive solutions can be more complex but offer the potential to provide traction across a larger range of terrain.

In this work, we present a mobile robotic system that utilizes a vehicle-mounted manipulator to physically adapt the robot with different anchors, each optimal for a unique surface to increase vehicle traction. Specifically, this work explores how a wheeled robot can increase its payload capacity on various terrain with swappable anchors. This work expands on the previously explored swappable propulsors framework [19], [20], which enables different modes of locomotion by swapping propulsors using a vehicle-mounted manipulator. This work presents four unique anchor designs, each of which increases vehicle traction on a specific surface, and experimentally validates them. The experimental results illustrate how this approach can increase the overall payload capacity of a system on various terrain by increasing the effective coefficient of friction. We delineate how we can use the manipulator to autonomously localize the payload using a visual sensor, attach the payload to the vehicle using a permanent-magnet-based payload lock, and pull up to $38\times$ its body mass using the anchors.

III. SWAPPABLE ANCHOR FRAMEWORK

A. Functional Requirements

This section outlines the general functional requirements needed for the swappable anchor framework. Swappable anchors are devices that engage with a given surface to increase the coefficient of friction. Specifically, the anchor must be able to handle resistive forces from the payload, must be detachable, and must not consume energy. Swappable anchors offer solutions for increasing vehicle traction on various surfaces, and a few examples are shown in Figure 2. This figure illustrates how anchors can be designed to increase friction on (a) rough surfaces with asperities, (b) wet, muddy surfaces, (c) flat, smooth surfaces, and (d) soft, granular surfaces. The presented framework assumes that a mobile robot can store and carry multiple sets of swappable anchors, each associated

with a particular surface. We defined the following functional requirements for an efficacious swappable anchor design:

1) **Increase coefficient of friction between the system and the surface.** The anchors should enable a mobile robot to pull loads that are substantially greater than the robot's mass. Once engaged, the surface contact of the anchors should increase the overall vehicle traction.

2) **High-holding force and zero power consumption during engagement.** When engaged, the anchors must remain attached to the robot to maintain effective contact with the surface. Maintaining the engagement of the anchoring device should not require energy consumption.

3) **Low force detachment using manipulation.** To pull loads on various surfaces, anchors must be swappable using a vehicle-mounted manipulator. Manipulators have force/weight limitations, so the detachment force should be sufficiently less than the minimum holding force.

4) **Reversible Anchoring.** The mobile robot should be able to unanchor itself. This is needed to maintain robot mobility and enable payload transportation across various surfaces.
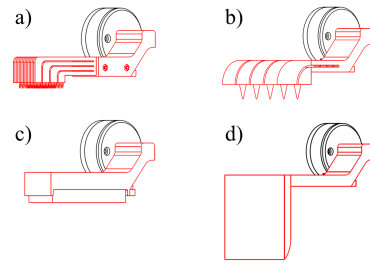

Fig. 2. a) Microspine anchor; b) macrospine anchor; c) adhesive-rubber anchor; d) sand anchor. This figure illustrates how a range of swappable anchors can be designed for a particular surface. A range of swappable anchors (red) can be attached to a single housing (black).

B. Permanent Magnets with Mechanically Constraining Steel Surface Mounts

The mounting design described in the swappable propulsor framework [19], [20] satisfies the aforementioned functional requirements 2) and 3). As a result, this work adapts the swappable propulsor mounting design onto swappable anchors to enable reliable attachment and easy detachment with permanent magnets and geometric features.

To ensure reliable attachment, this mechanism leverages permanent magnets with ferrous steel surface mounts and T-slots. Permanent magnets with ferrous steel enable large attachment forces with low added mass and zero static power consumption. The design limits undesired detachments in unwanted directions by using mating features with T-slots and mechanical frames. For easy detachment, the vehicle-mounted manipulator is used to overcome the magnetic attachment force. By exploiting geometric features, we can reduce the amount of force needed to overcome the attachment force. Specifically, we can use a large moment arm to decrease the magnetic attachment force by creating an air gap.

C. Anchor Design for Payload Transport

We can enable reversible anchoring by attaching anchors to the center actuators. The anchors can be rotated to engage the surface during payload pull and disengaged during motion. To maximize payload capacity, the swappable anchor must utilize an optimized surface contact with a high coefficient of friction, resist vehicle displacement, and maintain reliable contact with the surface. We can ensure the anchors maintain contact with the surface without any energy consumption by shaping the anchor such that the tensile force from the winch causes the anchors to dig deeper into the surface. Figure 3 illustrates the design of the anchor used in this study and the forces in play during a stable payload pull.
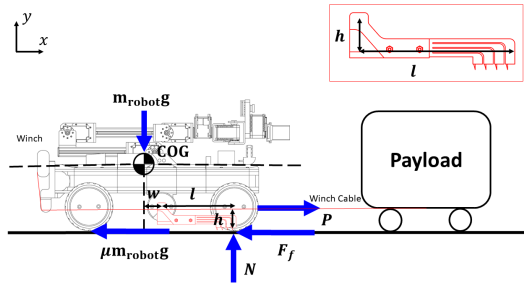

Fig. 3. Force diagram representation of the vehicle pulling the payload using the winch.

$$\sum F_x = 0 = \mu m_{robot}g + F_f - P \qquad (1)$$

$$\sum F_y = 0 = m_{robot}g - N \qquad (2)$$

$$\sum M_{actuator} = 0 = m_{robot}gw + Nl - (F_f + \mu m_{robot}g)h \qquad (3)$$

$$\sum M_{anchor} = 0 = m_{robot}g(w + l) - Ph \qquad (4)$$

μ represents the coefficient of friction of the tires. m_{robot} and P represent the mass of the robot and the force of the payload respectively. We use h to represent the height of the anchor. l represents the length of the anchor and w is the horizontal distance from the center actuator to the center of mass. We denote F_f as the friction force and N as the normal force of the wheels and anchors.

The static force balance for the x and y directions are provided in 1 and 2. Equation 3 depicts moments about the center actuator during payload pull. When pulling substantially heavy loads, the friction forces may be large enough to generate a clockwise moment and results in the anchor digging into the surface.

While this design can improve anchoring, the moment around the tip of the anchor can cause the vehicle to flip over. Flipping over can degrade performance and may prevent the robot from recovering its mobility. Therefore, we need to determine geometric parameters that prevent flipping under expected loads.

Given a vehicle with known dimensions and a goal maximum payload, we can select the dimensions of the anchor, h, l, such that the moment caused by the payload does not flip the vehicle. Equation 4 denotes the condition that must be maintained to ensure the tensile force from the winch does not create a moment and lift the robot during the pull. Substituting and rearranging Equation 4, we can obtain the set of possible dimensions for h and l that can be used to prevent flipping under expected loads. This is denoted in Equation 5.

$$\frac{m_{robot}g}{P} = \frac{h}{w + l} \qquad (5)$$

IV. TAILORED OPTIMIZED TRACTION MECHANISMS FOR VARIOUS TERRAIN

Varying terrain conditions are each associated with an optimal traction mechanism. We identify optimized traction mechanisms from the existing literature and customize them for swappable use on a mobile robot.

A. Hard Rough Surface Contact Design

For hard rough surfaces, the existing literature has already provided an excellent traction mechanism. Specifically, microspines are effective surface contacts for increasing friction on hard, rough surfaces such as concrete or rocky terrain [10]. Microspines consist of one or more hooks embedded in a rigid frame with a compliant suspension system. By arraying tens or hundreds of these microspines, large loads can be supported and shared between many attachment points. Since each spine has its own suspension structure, it can stretch and drag relative to its neighbors to find a suitable asperity to grip. While most previous microspine works have focused on low normal force (climbing applications) or low total force (microbots), our application focuses mainly on high coefficient of friction while supporting large normal loads. This will maximize ground friction and bear high tensile loads from the winch during payload pulling.

To create a microspine anchor that can efficiently and effectively increase the friction between the vehicle and the surface, we follow the design principles detailed in works [18], [21]. Since much of the design and analysis of the microspines have been researched already, we do not repeat them here. The design of the microspine anchor used in this work is shown in Figure 4(a).

B. Wet Cohesive Surface Contact Design

Wet, cohesive surfaces such as mud, forest soils, marshes, littorals, estuaries, and wet fields are ubiquitous in nature. These surfaces have properties changing in space and time, due to their infinite number of possible compositions. Therefore, deriving a general model for mud is complex and unpractical. Instead, we design a solution based on existing literature and empirically evaluate its efficacy and performance. In this work, we present a macrospine surface contact solution that enables increased stationary vehicle traction.

Macrospines consist of steel hooks with larger radius tips in the millimeter range. These millimeter range spikes, in
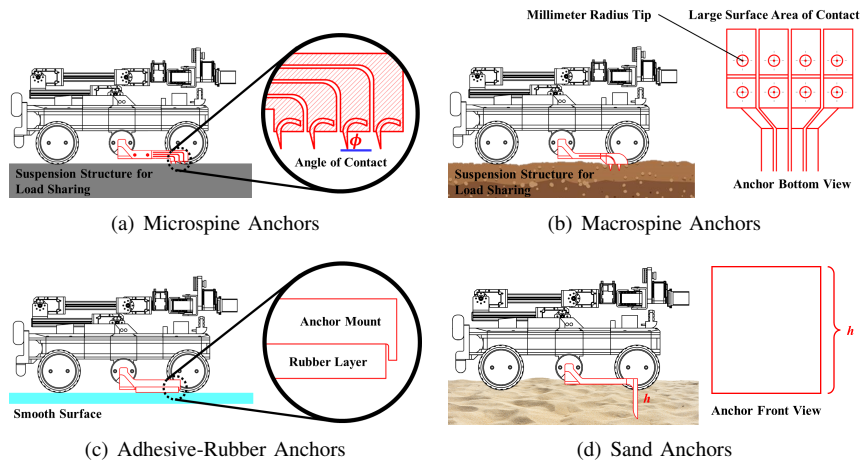
Fig. 4. Anchor designs explored in this work. (a) Each layer has 4 microspines embedded. To handle the maximum shear load, the microspines are inserted such that the angle of contact, $\phi = 90 \sim 155\,\mathrm{deg}$. (b) Macrospine anchors use millimeter range radius tip spikes to pierce into wet, cohesive surfaces. Once submerged, large surface area of contact minimizes erosion of the surface. (c) Adhesive-rubber anchors consist of two layers, the anchor mount, and the rubber layer. (d) Sand anchors utilize greater insertion depth (h) to result in higher vehicle traction.

comparison to microspines, can pierce deeply through the cohesive terrain without completely destroying the cohesion of the surface. Once the spikes are submerged, the anchor makes large surface area of contact with mud, holding any erosion that may occur in place.

Results from [22], [23] show that the relationship between submersion and friction on mud can be approximated by a linear relationship whose slope is dependent on water content. Hence, we require a surface contact that can sink into the surface for high vehicle traction. These studies also illustrated how too stiff or too soft contact does not provide as much support force as intermediate stiffness. If the contact is too stiff, it either erodes the surface or slips. Too soft, it loses traction. Therefore, our proposed design uses a suspension structure much like the microspines to passively distribute the load across spikes and to prevent erosion of the surface. The design of the macrospine anchor used in this work is shown in Figure 4(b).

C. Smooth Surface Contact Design

Studies from [18] have demonstrated that high-friction, long-wearing rubber is effective in supporting large normal loads with a high coefficient of friction on flat smooth surfaces. This work utilizes abrasion-resistant polyurethane rubber as surface contact. The design of the adhesive rubber anchor is shown in Figure 4(c).

D. Granular Surface Contact Design

To increase vehicle traction on soft, granular media such as sand, we follow the principles outlined in [17] to design our surface contact. The study illustrates how an anchoring device can be utilized to increase insertion depth, h, which results in increased resistive force. Greater insertion depth leads to larger normal loads with a higher coefficient of friction. The design principles suggest two methods for maximizing insertion depth, static insertions, and dynamic impact. The

static insertions method is well aligned for this study, due to the anchor design. The winch tension causes the anchors to dig deeper into the surface, increasing insertion depth. The design of the sand anchor is shown in Figure 4(d).

V. IMPLEMENTATION

This section describes the implementation of this new approach to payload transport. The custom prototype vehicle described in this work is designed to increase the overall payload capacity of the system across various terrain using four different swappable anchors. In addition, we describe a high-level planner that is used to demonstrate payload transport through autonomous payload attachment.

A. Prototype Vehicle

This work utilizes a four-wheeled vehicle with two actuators extruding at the center of the chassis for reversible anchoring. The prototype vehicle can carry two pairs of anchors (one on the chassis storage space, and the other on the actuators). The prototype vehicle is shown in Fig. 5. The wheels are driven by $50:1$ metal geared $12V$ DC motors. The center actuators are driven by $150:1$ metal geared $12V$ DC motors. The wheels are $105mm$ wide. Rubber tires are used on the four wheels. The vehicle frame is made of a combination of Delrin and Ultimaker Tough PLA and was fabricated using an Ultimaker S5 printer. The vehicle prototype is $465mm$ long, $320.8mm$ wide, and $204.8mm$ tall. The entire system has a mass of approximately $7kg$. 1/10 Warn 8274 Winch is installed at the rear.

B. Electronics

The low-level control of the entire robot system (vehicle and manipulator) is done with an Arduino MEGA 2560 microcontroller and a U2D2 controller (shown in Fig. 6). High-level planning is enabled by the Raspberry Pi 3B+ using ROS. The robot is powered by an 11.1V, 5000 mAh
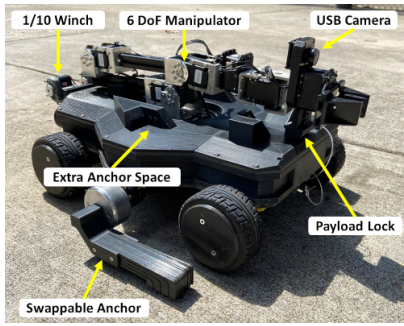
Fig. 5. Physical prototype vehicle used in this study. A 6 DoF vehicle-mounted manipulator with a USB camera is used to localize the payload, attach the payload to the vehicle, and swap anchors. The swappable anchor is used with the payload lock to pull a load using the 1/10 Warn 8274 winch installed at the rear. There is extra anchor space on top of the chassis to store a second set of anchors.

lithium-ion battery. The winch is driven by a Cytron Dual Channel 10 A DC motor driver. Each locomotive actuator is controlled using a custom motor control board. This board takes in the encoder and hall-effect sensor data and uses a Texas Instruments DRV8871 motor driver to control the motor. Control and communications are performed with an ATMega 328p microcontroller located on each motor control board. The motor controllers communicate with the central microcontroller using I2C. This enables position and velocity control over each of the six motors.
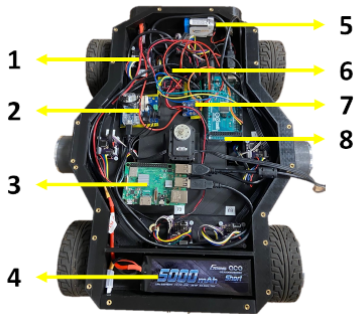

Fig. 6. View of the internal components of the prototype vehicle. 1) Custom-built I2C motor controller board; 2) U2D2 Controller; 3) Raspberry Pi 3B+; 4) 11.1V Lithium Ion Battery; 5) 9V battery; 6) Winch Motor Controller; 7) INA260 DC Current Sensor; 8) Arduino MEGA 2560.

C. Vehicle-Mounted Manipulator

This work utilizes a 6-degree-of-freedom (DoF) manipulator mounted at the center of the vehicle. The manipulator is comprised of three Dynamixel MX-106 servos, two Dynamixel MX-28 servos, and two Dynamixel AX-12A servos. A parallel-jaw gripper driven with an AX-12A servo was designed. The gripper is 3D printed and is rated for a holding force of $4.91N$. Arducam B0203 USB camera is mounted on the gripper.

The manipulator can be used for other purposes beyond swapping propulsors. This can include sampling the environment, localizing the payload using the camera, and attaching

the payload to the vehicle. The maximum payload of the manipulator is $400g$.

D. Swappable Anchors

Four different anchors are fabricated based on the surface contact designs presented in the previous section. The anchors are made of Ultimaker Tough PLA and were fabricated using an Ultimaker S5 printer.

The mounting hub on the center actuators, which house the swappable anchors, are made of Ultimaker Tough PLA and 6061 aluminum. The T-slot mount can withstand up to $56N$. The T-slot opening is covered with a layer of $0.635mm$ thick 430 stainless steel to enable magnetic attachments.

Two $6.4mm$ nickel-plated neodymium magnets, each rated for a pull force of $5.4N$, are embedded in each anchor. If the manipulator were to detach the anchor normal to the surface, it would need to exert $9.5N$ of force. The force needed to tilt the anchor is roughly $0.2N$. Once tilted, the detachment force is greatly reduced and is roughly $0.2N$. It takes roughly $1.8N$ to slide the anchor on the surface. These forces are measured experimentally.

1) Microspine Anchor: Each microspine is attached to a mounting layer with 3D printed PLA piece. The microspines are inserted mid-print at 90 to 155 degrees and then printed over. Microspines inserted at 90 to 155 degrees demonstrated maximum pull performance with a spring constant of 0.9 kN/m for a single layer. #10 carbon steel fish hooks are cut in shape to be used as microspines. A pair of anchors consist of 28 layers with a total of 112 microspines.

2) Macrospine Anchor: Each suspension layer is embedded with $15mm$ stainless steel US standard pyramid spikes. The macrospine anchor consists of a total of 8 spikes.

3) Adhesive-Rubber Anchor: Each anchor mount is attached with a $101.6mm$ x $25.4mm$ x $12.7mm$ abrasion-resistant polyurethane rubber rated at 70 Durometer.

4) Sand Anchor: The sand anchor uses $90mm$ x $90mm$ x $10mm$ Delrin plates to provide an insertion depth of $90mm$.

E. Enabling Autonomous Payload Transport

A critical use case for the vehicle-mounted manipulator is to allow for the autonomous retrieval of target payloads. With a camera-equipped 6 DoF arm, the robot is able to scan its surrounding environment and identify target payloads using fiducial markers. The robot can then approach the payload and attach a magnetic payload lock that allows the winch to pull the load securely.

High-level motion planning, trajectory execution, and actuation of the manipulator are run on ROS using the onboard Raspberry Pi. Tracking of fiducial markers is achieved with the open-source AR-tag tracking library Alvar. The robot performs basic localization by calculating the Euclidean distance to marker reference frames and navigates toward the payload with a simple motion controller. Using the reference frame of the AR tag, the system determines the desired end-effector orientation for proper lock placement and plans a motion path using the default optimization of minimal path length. These

manipulation tasks are performed through the MoveIt motion planning framework and using the Open Motion Planning Library (OMPL) planner. Once the payload lock is securely attached, the robot proceeds with transporting the payload using the winch and anchoring system. The state-machine of our planning scheme can be seen in Figure 7. The full demonstration of the autonomous payload transport capability is shown in Fig. 8 and the accompanying video [24].
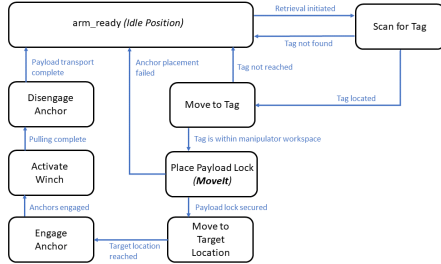

Fig. 7. ROS high-level planner state-machine chart used to demonstrate autonomous payload attachment and transport in this study.

VI. Performance

A. Increasing Friction to Transport Heavy Payloads

Outdoor testing was performed on surfaces readily available on Georgia Tech main campus. A series of experiments were performed to quantify and compare the performance of our prototype's maximum innate capability (without anchors) to pull payloads to the maximum payload capacity with swappable anchors. The experiments are shown in the accompanying video [24] and in Figure 10.

First, to quantify the innate capability to pull payloads on different surfaces, we conducted a series of static friction tests by attaching a precision spring force gauge to our prototype vehicle. We define a vehicle's maximum innate traction to be the point at which the vehicle slips during a wheels-locked condition. For our system, the wheels are locked using position control on the drive motors. Our initial tests measured the resistive force at the onset of displacement. The tests measured the forces on five different surfaces (concrete, polysynthetic ice, sand, mud, and grass) by pulling with the spring force gauge. Once the vehicle was displaced, the experiment was stopped. The peak force was verified via video analysis and recorded for a set of different surfaces. Each surface was tested with 20 trials. With the resistive force measurements, we obtained the normalized coefficient of friction of each condition on each surface. The results can be seen in Figure 9(a).

Results from Figure 9(a) indicate that innate vehicle traction using locked wheels is consistent on concrete, mud, and grass with an averaged normalized coefficient of friction of approximately 1.06. However, on surfaces with a lower coefficient of friction such as polysynthetic ice and sand, vehicle traction degrades drastically. This clearly illustrates the need for various surface contact solutions to increase vehicle traction during payload pull. We conducted further experiments using microspine, macrospine, adhesive-rubber,

and sand anchors on 5 different surfaces. These conditions did not involve using motor position control. The results are shown in Figures 9(b), 9(c), 9(d), and 9(e) respectively.

Compared to the vehicle's innate traction, the microspine anchors demonstrated up to twice as much resistive force on concrete and grass with an increased coefficient of friction of 1.42 and 2.02 respectively. On polysynthetic ice, sand, and mud, the microspine anchors did not show much improvement.

Macrospine anchors resisted more load on mud and sand with an increased coefficient of friction of 1.87 and 1.89. The adhesive-rubber anchors were able to withstand six times more load on polysynthetic ice with a normalized coefficient of friction of 1.55.

Sand anchors showed three times more resistive capability on sand with an increased coefficient of friction of 1.96. These results illustrate how each anchoring device improves vehicle traction on its intended surface.

Figure 9(f) compares the vehicle's innate pulling capability to an optimal anchor's capability. Note that no single design provides excellent performance across the terrain. However, by swapping anchors, a system can improve its overall payload capacity by using an optimal anchoring solution.

We also evaluated the overall performance of the optimized swappable anchors integrated with our system. Our tests consisted of measuring the maximum payload mass quantity that the vehicle could pull using the winch before the wheels began to slip. For consistency, the same surfaces were used, and the payload was placed on a wheeled cart. Maximum payload testing was conducted by placing a known weight on the cart and then having the winch pull the payload. The payload mass was increased by 5kg until the anchors failed. For this and subsequent tests, failure was defined as the robot rover displacing a full body length. The results are shown in Table I.

The fully integrated system (7kg mass) was able to pull 38 times the body mass on concrete, 28 times on ice, 8 times on sand, and 16 times on mud and grass.

TABLE I
Maximum Payload Capacity with Optimized Swappable Anchors

Concrete	Ice	Sand	Mud	Grass
265kg	195kg	60kg	115kg	115kg

B. Using Manipulation to Increase Payload Capacity Across Various Surfaces

The last step is to validate and demonstrate the actual physical adaptation. OMPL planner was used to demonstrate the swapping of the anchors. The trajectory planner was given specific Cartesian waypoints to execute the slide and tilt motion needed to attach/detach the anchors from the mounting hubs. Closed-loop position control of the propulsor mounts is used to make sure they are aligned correctly. The anchors were designed with handles that could mate with the gripper for

(a) Survey Environment and Localize Payload

(b) Approach Payload

(c) Grasp Payload Lock

(d) Attach Payload to Vehicle

(e) Deploy Anchors and Pull Payload
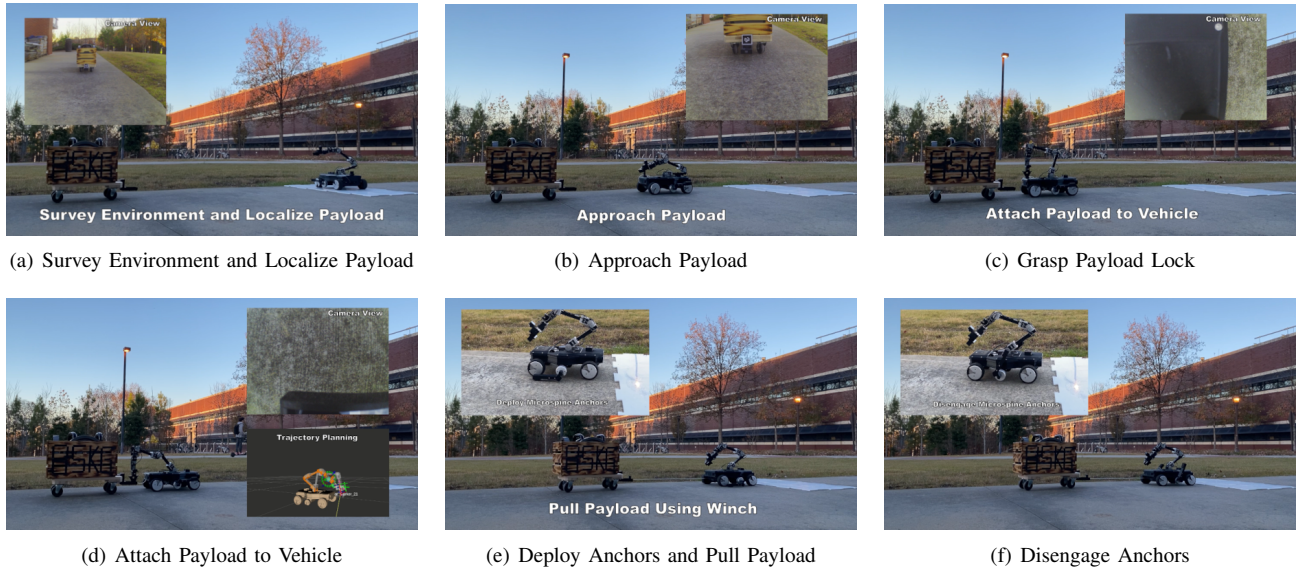
(f) Disengage Anchors

Fig. 8. Photographic illustration of the autonomous payload transport. (a) The robot localizes the fiducial marker on the designated payload. (b) The fiducial marker provides the relative position, and the system is then able to approach the payload. (c) The robot uses the manipulator to grasp the payload lock. (d) The robot plans a trajectory to attach the payload to the vehicle using marker frames. (e) The robot retreats and deploys the anchors onto the ground to displace the payload using the winch. (f) Lastly, the anchors are disengaged.

(a) Innate Vehicle Traction

(b) Microspine Anchors

(c) Macrospine Anchors

(d) Adhesive-Rubber Anchors

(e) Sand Anchors

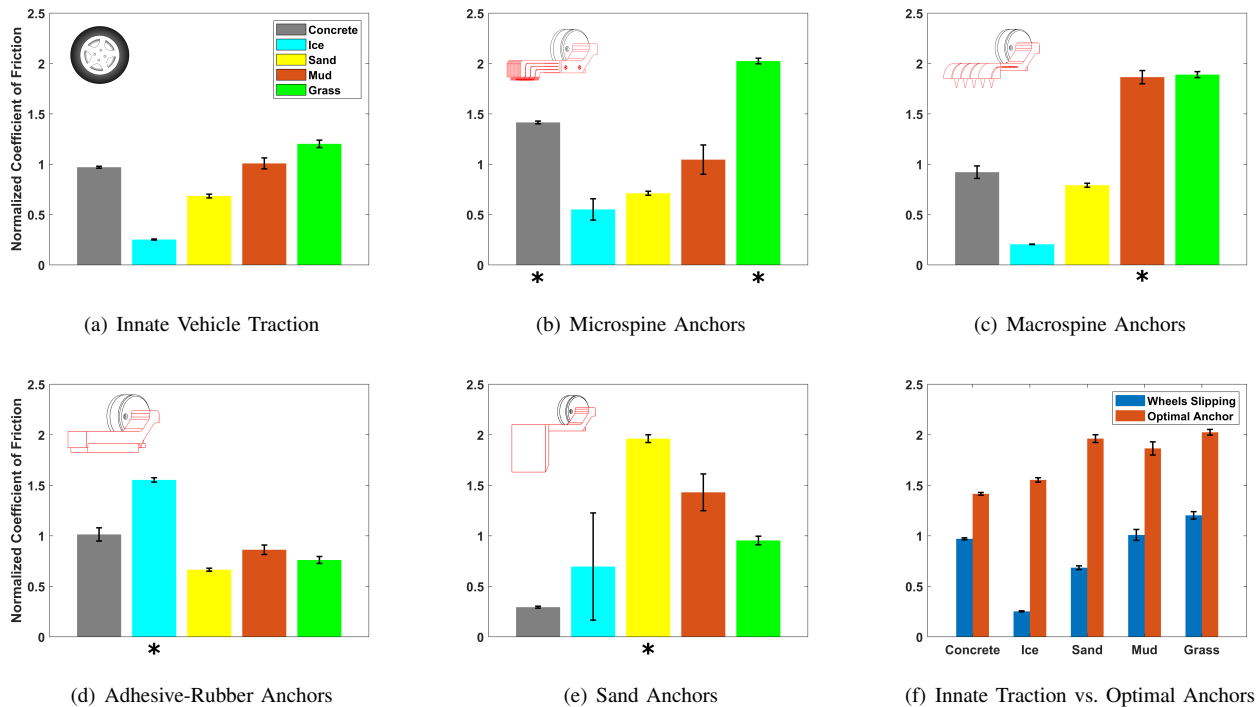(f) Innate Traction vs. Optimal Anchors

Fig. 9. Bar plots showing the normalized coefficient of friction of each condition on 5 different surfaces. The optimal surface for each anchor is marked with an asterisk below. (a) Normalized coefficient of friction values using the vehicle's innate traction. (b) Normalized coefficient of friction values using microspine anchors. (c) Normalized coefficient of friction values using macrospine anchors. (d) Normalized coefficient of friction values using adhesive-rubber anchors. (e) Normalized coefficient of friction values using sand anchors. (f) Normalized coefficient of friction values comparing vehicle's innate traction vs. optimal anchors.

Fig. 10. Terrain testing across multiple surfaces. (1) Microspine anchors pulling up to $265kg$ on concrete. (2) Microspine anchors pulling up to $115kg$ on grass. (3) Macrospine Anchors pulling up to $115kg$ on mud. (4) Adhesive-rubber anchor pulling up to $195kg$ on polysynthetic ice. Sand Anchors pulling up to $60kg$ is shown in Figure 1.

consistent grasping at a fixed orientation. The entire swapping process takes $100s$. The demonstration of swapping two sets of anchors is illustrated in the accompanying video [24].

VII. Conclusion

In this work, we presented a mobile robotic system that utilizes a vehicle-mounted, multipurpose manipulator to physically adapt the robot with unique anchors suitable for a particular terrain to increase payload capacity. This work presented "swappable anchors", which can be easily attached/detached to adapt the vehicle using permanent magnets. Four unique anchor designs were introduced and experimentally evaluated on five different surfaces. The experimental results illustrated how this approach can increase the overall payload capacity of a system on various surfaces by increasing the overall effective coefficient of friction. This study also experimentally demonstrated how we can use the manipulator to autonomously localize the payload using a visual sensor, attach the payload to the vehicle using a permanent-magnet-based payload key/lock, and pull several times its body mass using the swappable anchors. The proposed methods can enable ground robots to be more adaptive, robust, and autonomous. Instead of requiring redesign, the robotic system can modify itself relatively quickly and handle new terrain or conditions.

VIII. Acknowledgments

References

[1] D. L. Christensen, E. W. Hawkes, S. A. Suresh, K. Ladenheim, and M. R. Cutkosky, "μtugs: Enabling microrobots to deliver macro forces with controllable adhesives," in *2015 IEEE International Conference on Robotics and Automation (ICRA)*. IEEE, 2015, pp. 4048–4055.

[2] A. Parness, N. Abcouwer, C. Fuller, N. Wiltsie, J. Nash, and B. Kennedy, "Lemur 3: A limbed climbing robot for extreme terrain mobility in space," in *2017 IEEE International Conference on Robotics and Automation (ICRA)*. IEEE, 2017, pp. 5467–5473.

[3] M. P. Murphy and M. Sitti, "Waalbot: An agile small-scale wall-climbing robot utilizing dry elastomer adhesives," *IEEE/ASME transactions on Mechatronics*, vol. 12, no. 3, pp. 330–338, 2007.

[4] E. W. Hawkes, E. V. Eason, A. T. Asbeck, and M. R. Cutkosky, "The gecko's toe: Scaling directional adhesives for climbing applications," *IEEE/ASME transactions on mechatronics*, vol. 18, no. 2, pp. 518–526, 2012.

[5] J. He, Y. Sun, L. Yang, J. Sun, Y. Xing, and F. Gao, "Design and control of tawl—a wheel-legged rover with terrain-adaptive wheel speed allocation capability," *IEEE/ASME Transactions on Mechatronics*, vol. 27, no. 4, pp. 2212–2223, 2022.

[6] Z. Li, Z. Li, L. M. Tam, and Q. Xu, "Design and development of a versatile quadruped climbing robot with obstacle-overcoming and manipulation capabilities," *IEEE/ASME Transactions on Mechatronics*, 2022.

[7] J. Xiao, B. Li, K. Ushiroda, and Q. Song, "Rise-rover: A wall-climbing robot with high reliability and load-carrying capacity," in *2015 IEEE International Conference on Robotics and Biomimetics (ROBIO)*. IEEE, 2015, pp. 2072–2077.

[8] B. Jin, S. Ye, J. Su, and J. Luo, "Unknown payload adaptive control for quadruped locomotion with proprioceptive linear legs," *IEEE/ASME Transactions on Mechatronics*, 2022.

[9] M. Hutter, C. Gehring, D. Jud, A. Lauber, C. D. Bellicoso, V. Tsounis, J. Hwangbo, K. Bodie, P. Fankhauser, M. Bloesch *et al.*, "Anymal-a highly mobile and dynamic quadrupedal robot," in *2016 IEEE/RSJ International Conference on Intelligent Robots and Systems (IROS)*. IEEE, 2016, pp. 38–44.

[10] A. T. Asbeck, S. Kim, M. R. Cutkosky, W. R. Provancher, and M. Lanzetta, "Scaling hard vertical surfaces with compliant microspine arrays," *The International Journal of Robotics Research*, vol. 25, no. 12, pp. 1165–1179, 2006.

[11] W. Ruotolo, F. S. Roig, and M. R. Cutkosky, "Load-sharing in soft and spiny paws for a large climbing robot," *IEEE Robotics and Automation Letters*, vol. 4, no. 2, pp. 1439–1446, 2019.

[12] M. J. Spenko, G. C. Haynes, J. Saunders, M. R. Cutkosky, A. A. Rizzi, R. J. Full, and D. E. Koditschek, "Biologically inspired climbing with a hexapedal robot," *Journal of field robotics*, vol. 25, no. 4-5, pp. 223–242, 2008.

[13] M. A. Estrada, S. Mintchev, D. L. Christensen, M. R. Cutkosky, and D. Floreano, "Forceful manipulation with micro air vehicles," *Science Robotics*, vol. 3, no. 23, 2018.

[14] A. L. Desbiens, A. Asbeck, and M. Cutkosky, "Hybrid aerial and scansorial robotics," in *2010 IEEE International Conference on Robotics and Automation*. IEEE, 2010, pp. 72–77.

[15] J. Park, H.-W. Park *et al.*, "Design of anti-skid foot with passive slip detection mechanism for conditional utilization of heterogeneous foot pads," *IEEE Robotics and Automation Letters*, vol. 4, no. 2, pp. 1170–1177, 2019.

[16] K. Carpenter, N. Wiltsie, and A. Parness, "Rotary microspine rough surface mobility," *IEEE/ASME Transactions on Mechatronics*, vol. 21, no. 5, pp. 2378–2390, 2015.

[17] J. Fernandez and A. Mazumdar, "Tail-based anchoring on granular media for transporting heavy payloads," *IEEE Robotics and Automation Letters*, vol. 6, no. 2, pp. 1232–1239, 2021.

[18] C. C. Berdan, B. G. Johnson, and E. W. Hawkes, "Microspine-rubber composite for high friction on smooth, rough, and wet surfaces," in *2021 IEEE/RSJ International Conference on Intelligent Robots and Systems (IROS)*. IEEE, 2021, pp. 7384–7390.

[19] R. Kim, A. Debate, S. Balakirsky, and A. Mazumdar, "Using manipulation to enable adaptive ground mobility," in *2020 IEEE International Conference on Robotics and Automation (ICRA)*. IEEE, 2020, pp. 857–863.

[20] R. Kim, V. Madabushi, E. Dong, and A. Mazumdar, "Increasing mobile robot efficiency and versatility through manipulation-driven adaptation," *Journal of Mechanisms and Robotics*, vol. 13, no. 5, p. 050906, 2021.

[21] M. Martone, C. Pavlov, A. Zeloof, V. Bahl, and A. M. Johnson, "Enhancing the vertical mobility of a robot hexapod using microspines," *arXiv preprint arXiv:1906.04811*, 2019.

[22] S. Godon, A. Ristolainen, and M. Kruusmaa, "An insight on mud behavior upon stepping," *IEEE Robotics and Automation Letters*, vol. 7, no. 4, pp. 11 039–11 046, 2022.

[23] J. Y. Wong, *Terramechanics and off-road vehicle engineering: terrain behaviour, off-road vehicle performance and design*. Butterworth-heinemann, 2009.

[24] R. Kim, E. Diller, E. Harkonen, and A. Mazumdar, "Increasing mobile robot payload capacity through multipurpose manipulation," https://youtu.be/0chaPN2KOwA, accessed: 2022/12/16.